Isotope effects on the electronic excitations and phonons in semiconductors

M. Cardona, C.H. Grein, H.D. Fuchs and S. Zollner

Max-Planck-Institut für Festkörperforschung, Heisenbergstr. 1, W-7000 Stuttgart 80, Germany

Changes in the average isotopic mass, $\overline{M}$, produce a trivial effect in the phonon spectra of monoatomic solids, i.e., the variation of phonon frequencies such as $\overline{M}^{-1/2}$. More sophisticated effects also appear. Effects on the frequencies of phonons and electronic excitations due to changes in the mean squared amplitude, $\langle u^2 \rangle$, which also varies like $\overline{M}^{-1/2}$, and effects of the mass fluctuations in isotopically mixed crystals are discussed. The latter can be represented by a complex self-energy whose real part corresponds to a frequency shift and its imaginary part to an increase in phonon linewidth.

1. Introduction

Among the various types of disorder in solids, isotopic disorder is perhaps the least conspicuous and most poorly investigated. Yet a material such as natural silicon contains three isotopes (^{28}Si, 92%; ^{29}Si, 5%; ^{30}Si, 3%) while germanium is composed of five different isotopes with abundances of the same order of magnitude (^{70}Ge, 20.5%; ^{72}Ge, 27.4%; ^{73}Ge, 7.8%; ^{74}Ge, 36.5%; ^{76}Ge, 7.7%). Isotopically pure materials are prepared nowadays by means of isotope separators, sometimes in large quantities. In particular, at the Kurchatov Institute (Moscow) several germanium isotopes with isotopic purities better than 95% are being separated. Large, high purity single crystals are being grown from these materials. They are used as neutrino (^{76}Ge) and as γ-ray detectors (^{70}Ge) [1].

The isotopic composition affects many of the physical properties of crystals. The effects can be classified into two categories: (i) effects of the individual isotopes, such as those due to their different nuclear magnetic moments or atomic masses, and (ii) effects of the isotopic disorder, in particular the atomic mass fluctuations in natural or isotopically mixed materials. In this paper, we discuss effects of both types on the electronic and vibronic properties of the solid which should be a paradigm for such studies, namely crystalline germanium. Besides the effects discussed here, isotopic disorder is known to be mainly responsible for scattering of long wavelength acoustic phonons [2]. Also, changes in isotopic mass have been recently shown to lead to small but observable changes in the lattice constant of crystals (germanium) [3].

The data presented here were obtained for three *n*-type germanium crystals. Two of them (natural Ge and isotopically enriched ^{76}Ge) were intrinsic at room temperature $N_d - N_a \approx 10^{14}$ cm^{-3}) while the other (isotopically enriched ^{70}Ge) had $N_d - N_a \simeq 7 \times 10^{16}$ and independent values of N_d and N_a in the mid 10^{17} cm^{-3} range. The isotopic composition of these samples is given in table 1. Among the phenomena presented and discussed here are the dependence of the E_1 and

Table 1
Isotopic composition of isotopically enriched ^{70}Ge, ^{76}Ge, and natural Ge used in this experiment

M	Atomic percent of the various isotopes					g (10^{-5})
	70	72	73	74	76	
^{70}Ge	95.9	3.8				2.976
$^{72.6}$Ge	20.5	27.4	7.8	36.5	7.1	58.745
$^{75.6}$Ge		0.1	0.23	13.7	86.0	8.797

$E_1 + \Delta_1$ electronic gap frequencies on isotopic mass. These gaps occur in germanium at ~ 2.2 and 2.4 eV and contribute largely to the strength of the polarizability. Their connection with the band structure of germanium was identified by Jan Tauc in 1960 [4]. This seminal discovery had important consequences for optical spectroscopy and band structure studies of semiconductors. One of the authors (M.C.) has devoted a good deal of his career to the investigation of phenomena related to that discovery and would like to express here his gratitude to Jan Tauc, and admiration for his pioneering work.

2. Isotopic effect on the frequencies and widths of the E_1 and $E_1 + \Delta_1$ transitions

2.1. The E_1 and $E_1 + \Delta_1$ gaps

These transitions are much stronger than those at the direct edge of germanium (E_0 and $E_0 + \Delta_0$, 0.8–1.2 eV): the maximum absorption coefficient ($\alpha \sim 2 \times 10^5$ cm^{-1}) is an order of magnitude larger than that at E_0 which, in its turn, is two orders of magnitude larger than at the lowest indirect edge. At the time Tauc and co-workers wrote [4], the E_1 and $E_1 + \Delta_1$ direct transitions were believed to occur at the L-point of the Brillouin zone (edge of zone along the $\langle 111 \rangle$ directions) [5]. Shortly after, and following advances in band structure calculations, this assignment was confirmed [6], but also extended to include most other transitions between the top valence band and the lowest conduction bands along the $\langle 111 \rangle$ directions (Λ directions) throughout most of the Brillouin zone (BZ). These bands are nearly parallel throughout that region. The critical points for the corresponding interband transitions, which determine the lineshapes of the real and imaginary dielectric functions $\epsilon_1(\omega)$ and $\epsilon_2(\omega)$, are thus of two-dimensional type. Those lineshapes exhibit a logarithmic singularity at E_1 and $E_1 + \Delta_1$ (for ϵ_1) and a step for ϵ_2. Excitonic effects modify these lineshapes [7] in a way which can be studied with great accuracy by means of spectral ellipsometry [8]. The accuracy of digital ellipsometric data is so high that

frequency derivatives, usually up to the third, can be precisely calculated and fitted to theoretical lineshapes for two-dimensional critical points at E_1 and $E_1 + \Delta_1$. Among other lineshape parameters, the critical point energies and their Lorentzian broadenings are obtained in this manner. In the case of germanium they have been studied in detail vs. temperature [7] and heavy doping with shallow impurities [9]. The corresponding frequency and linewidth renormalizations can be regarded as real and imaginary parts of disorder-induced self-energies.

2.2. Renormalization of electronic states and interband transition gaps by electron–phonon interaction

The electronic states are normalized by their interaction with the phonon system. As a result, the frequencies of the interband critical points are modified (usually slightly reduced) [10] and their Lorentzian broadenings are enhanced [11]. The frequency shift is usually broken up into two contributions, the 'Debye–Waller' (also called Antončík–Brooks–Yu) terms and the self-energy or Fan terms [10,11]. The former correspond to the electron–two-phonon interaction Hamiltonian taken in first order perturbation theory, while the latter arise from the electron–one-phonon interaction in second order perturbation theory. For transitions in the 0–6 eV range, the latter are the only contributors to the linewidth, i.e., to the lifetime of the excitations. For a review, see ref. [12].

At high temperatures ($T > T_D$, the Debye temperature), all self-energy terms just mentioned become linear in T. At low temperatures, the T dependence flattens out. Neither the real (Σ_r) nor the imaginary (Σ_i) parts of the electron–phonon self-energies (from now one Σ_r is assumed to include the Debye–Waller term) vanish in general for $T \to 0$. However, Σ_i does vanish at the lowest absorption edge for $T \to 0$, since at these temperatures only phonon emission processes are possible and no energy-conserving final states are available (no excitation lower than the lowest, by definition). This does not need to occur at higher gaps such as E_1 and $E_1 + \Delta_1$.

2.3. Self-energies at $T \to 0$ and isotope shifts of the band gaps and widths

The electron–phonon-generated Σ_r in a monoatomic crystal can be written as [9]

$$\Sigma_r = A\langle u^2 \rangle = A\left(\frac{\hbar}{2M\bar{\omega}}\right)(1 + 2n(\bar{\omega})), \tag{1}$$

where M is the atomic mass (average mass in case of isotopic admixture), $n(\bar{\omega}) = [\exp(\hbar\bar{\omega}/kT) - 1]^{-1}$ is the Bose–Einstein statistical factor and $\bar{\omega}$ is an average phonon frequency ($\hbar\bar{\omega} = kT_D$). At high temperatures ($T > T_D$), eq. (1) yields a self-energy independent of isotopic mass, M, since $n \approx kT/\bar{\omega}$ and $\bar{\omega} \propto M^{-1/2}$. At low temperatures, however, eq. (1) leads to a significant isotopic effect on Σ_r: Σ_r is proportional to $M^{-1/2}$. In Ge, the high temperature regime is expected to occur at and above room temperature while the low temperature, isotope effect displaying case should occur for $T \lesssim 100$ K.

An expression analogous to eq. (1) should apply to Σ_i at all band gaps (i.e. critical points) higher than the lowest one. At the lowest gap, only phonon absorption processes contribute to Σ_i and eq. (1) must be replaced by

$$\Sigma_i = B\left(\frac{\hbar}{M\bar{\omega}}\right)n(\bar{\omega}), \tag{2}$$

which should also exhibit an isotope effect at low temperatures. At these temperatures, however, the linewidth may be very small and isotope-induced changes in Σ_i will probably be unobservable. Hence the E_1 and $E_1 + \Delta_1$ transitions are ideal for the investigation of isotope effects in the linewidth Γ (i.e., $-\Sigma_i$), while effects on Σ_r can also be observed at the lowest direct gap, E_0, and at the indirect gap, E_I [13].

2.4. Ellipsometric measurements of isotope effect at the E_1 and $E_1 + \Delta_1$ gaps of Ge

The spectroscopic ellipsometry measurements of the three Ge samples of table 1 were performed at 10 K and room temperature inside a cryostat with quartz windows nearly free of birefringence. The reflecting surfaces were (111) oriented and polished and etched using the proce-
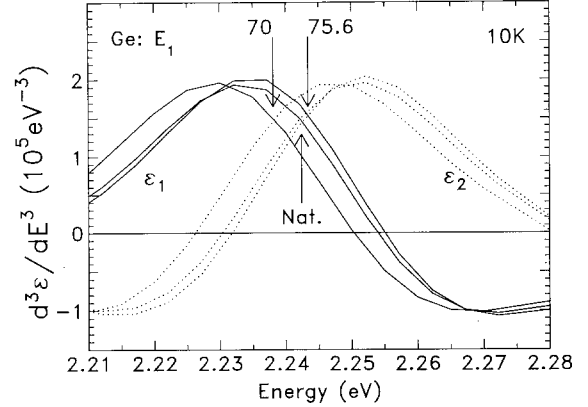

Fig. 1. Third order derivative spectra of the real (ϵ_1) and imaginary (ϵ_2) parts of the dielectric function of three germanium samples with different isotopic compositions (indicated by the arrows) around the E_1 critical point taken at 10 K. The vertical arrows show the positions of the critical point energies as determined from a lineshape analysis. The spectra have been multiplied by factors close to unity (0.8 ... 1.2) in order to have the same amplitude.

dure described in refs. [9] immediately before mounting them in the cryostat. The data obtained were, in all cases, very similar to those of ref. [9]. We show in fig. 1 the numerically generated third derivative spectra of ϵ_1 and ϵ_2 around E_1 for all three samples. The arrows indicate the critical point energies obtained from the fits to these spectra. Fits to second derivative spectra were also performed. While the critical point energies differed only slightly from those obtained for the third derivative fits (~ 5 meV), the relative shifts, however, were the same as shown in fig. 1 for the third derivatives. Note that the nearly rigid shifts from one sample to the other enable us to obtain rather reliable values for the 'isotopic' shifts. Slight deviations from the rigid shift at the high energy side of fig. 1 reveal changes in Γ which agree with the predictions of eq. (2): a larger Γ for lower M.

2.5. Discussion

A prediction of the change with M and comparison with the experimental results displayed in table 2 is easier for Σ_i than for Σ_r. The reason is

that the observed widths, Γ, are actually equal to $-\Sigma_i$, while Σ_r cannot be *directly* inferred from experiment. It must be estimated through a fit of the measured temperature dependence of E_1 and $E_1 + \Delta_1$ with eq. (1), and is thus strongly affected by uncertainties in $\bar{\omega}$. From eq. (2) we obtain directly the isotopic shifts in Γ given as $\delta\Sigma_i$ in table 2 with respect to the Σ_i of the natural material. We recall that the measured values of $\Gamma = -\Sigma_i$ agree reasonably well with those calculated from the 'Fan terms' using a realistic pseudopotential band structure and a lattice dynamics based on the bond charge model [11].

The interpretation of the measured $\delta\Sigma_r$ must be made by comparison with the calculated values of the zero-point $(T = 0)$ Σ_r [11]. We find from ref. [11] $\Sigma_r = 58$ meV averaged over the $\langle 111 \rangle$ points at which the E_1 and $E_1 + \Delta_1$ transitions occur (no spin–orbit splitting was included in these calculations, a fact which we now know does not significantly alter the values of Σ_r [14]). From this value of Σ_r and eq. (1) we find those of $\delta\Sigma_r$ listed in table 2.

It is strikingly apparent in table 2 that while the measured values of $\delta\Sigma$ for ^{76}Ge agree within the admittedly large error bars with the calculated ones, those for ^{70}Ge are considerably larger ($\sim$ a factor of 4) although they have the correct sign predicted by the isotopic shift theory. Since this sign is that which corresponds to increasing thermal agitation, i.e., disorder (the ^{70}Ge atoms vibrate with larger amplitude than the natural material $^{72.6}$Ge), we conjecture that our ^{70}Ge material contains a larger concentration of impurities than the other two samples known to have

$N_D \simeq 10^{14}$ cm^{-1}. The ^{70}Ge had not gone through the stringent 'Eagle Picher' purification process to which the other two samples had been subjected. We actually know that for our ^{70}Ge $N_D - N_A \simeq 7 \times 10^{16}$ cm^{-3}. In the absence of compensation (i.e., $N_A \ll N_D$), the corresponding donor concentration would have an unobservable contribution to Σ_r (≤ 0.5 meV) and to $\Gamma = -\Sigma_i$ (≤ 0.5 meV) [9]. We conclude that this sample must be strongly compensated (which was supported by IR-transmission data), with $N_D \simeq N_A = 5 \times 10^{17}$ cm^{-3} [7]. We note the possibility of using disorder-induced critical point shifts for an estimate of the degree of compensation in samples for which N_D and N_A are not separately known.

Effects of isotopic substitution have also been recently observed for the frequency of the lowest direct and indirect gaps of germanium [13] and for emission lines related to the indirect gap of diamond [15]. The work in ref. [13] was performed for $^{72.6}$Ge (natural) and $^{75.4}$Ge. The indirect gap was found to be 0.90(5) meV larger in $^{75.4}$Ge than in $^{72.6}$Ge, while the direct one (E_0) was 1.25(5) eV larger. The signs of these shifts agree with the predictions of eq. (1). Their magnitudes also agree with calculations based on the realistic lattice dynamics and band structures mentioned above: 1.28 meV for the indirect gap and 1.43 meV for the direct one [16], in rather good agreement with the experimental results. From these data, reliable estimates for $\Sigma_r(T = 0)$ can be obtained (average of theory and experiment: 63 meV for E_0, 51 meV for the indirect gap of natural $^{72.6}$Ge). We note that the effect of changes in lattice constant $(\Delta a_0/\Delta_0 < 2 \times 10^{-6})$

Table 2
Energies and Lorentzian widths (HWHM) of the E_1 and $E_1 + \Delta_1$ critical points of two isotopically enriched Ge samples (see table 1) and a natural one. The corresponding changes in self-energies, δE, are referred to the natural sample

$\overline{M}$	E_1 (meV)	$E_1 + \Delta_1$ (meV)	Γ_{E_1} (meV)	$\Gamma_{E_1 + \Delta_1}$ (meV)	$\delta\Sigma_r(E_1)$ (meV)	$-\delta\Sigma_i(E_1)$ (meV)	$\delta\Sigma_r(E_1 + \Delta_1)$ (meV)	$-\delta\Sigma_i(E_1 + \Delta_1)$ (meV)
^{70}Ge	2237.8(6)	2435.4(4)	35.1(3)	38.0(3)	$-4.4(18)$ [a] -1 [b]	2.1(4) [a] 0.5 [b]	$-4.9(12)$ [a] -1 [b]	1.9(8) [a] 0.6 [b]
$^{72.6}$Ge	2242.2(17)	2440.3(12)	33.0(3)	36.1(7)	0	0	0	0
$^{75.6}$Ge	2243.3(5)	2441.3(4)	32.6(2)	35.5(5)	1.1(18) [a] 1.35 [b]	$-0.4(4)$ [a] -0.8 [b]	1.0(12) [a] 1.35 [b]	$-0.6(9)$ [a] -0.8 [b]

[a] Experimental; [b] calculated.

[3] on the gaps can be estimated by using the well-known deformation potentials of the E_0 and indirect edges: they are negligible.

3. Isotope effects on the phonons of germanium

3.1. Introduction

Phonons are vibrations of the atomic cores and should therefore be highly sensitive to isotopic substitution. For an isotopically pure material, all phonon frequencies should be proportional to $M^{-1/2}$. This effect, which is rather trivial, has been investigated in ref. [13] for the L-phonons of $^{75.4}$Ge and $^{72.6}$Ge as observed in their indirect luminescence spectra. We note that isotopic substitution can be used to obtain information on eigenvalues as was recently done for the Cu–Ba vibrational modes of the high-T_c superconductor $YBa_2Cu_3O_7$ [17].

In the case of an isotopically disordered material, such as natural Ge, the phonon frequency vs. k and their disorder induced widths can be obtained by either perturbation theory or by means of the more sophisticated coherent potential approximation (CPA) which includes certain classes of perturbation diagrams to all orders [18]. First order perturbation theory is equivalent to the virtual crystal approximation (VCA): the phonon frequencies are not broadened by the disorder, only shifted as would correspond to a 'virtual crystal' with virtual atoms which have as a mass an arithmetic average, $\overline{M}$, of the isotopic masses M_i. Beside this also trivial effect, the fluctuations in the isotopic masses induced in second (and higher) order perturbation theory additional frequency shifts and broadenings which can be represented by a complex self-energy.

The isotopic fluctuations are usually expressed by the factor, g, defined as

$$g = \sum_i x_i \left(1 - \frac{M_i}{\overline{M}}\right)^2, \tag{3}$$

where x_i is the concentration of isotope i. The values of g for the samples under discussion are given in table 1. The self-energy due to the iso-

topic disorder is, in the self-consistent Born approximation, given by [18]

$$\Pi = \Pi_r + i\Pi_i, \tag{4a}$$

$$\Pi_r(\omega) \cong \frac{\omega^2 g}{24N} \sum_{q'j'} \frac{2\omega_{q'j'}}{\omega^2 - \omega_{q'j'}^2 - 2\omega_{q'j'}\Pi_r(\omega)} \tag{4b}$$

$$\Pi_i(\omega + \Pi_r(\omega)) \cong -\frac{\pi}{24}\omega^2 gRe\rho(\omega$$
$$-i\Pi_i(\omega + \Pi_r(\omega))) - \Gamma_p, \tag{4c}$$

where ρ is the phonon density of states, ω_{qj} is the frequency of a branch j phonon with wavevector q, N is the number of unit cells in the sample,
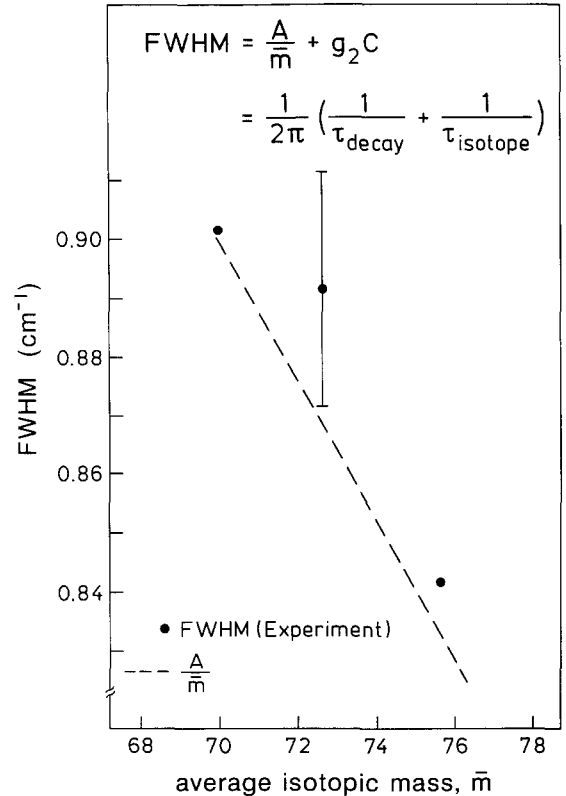

Fig. 2. Dependence of the FWHM (2Γ) on the average isotopic mass, $\overline{M}$, for the three germanium samples of table 1. The points are experimental, one of them including error bars. The dashed line represents the variation in 2Γ induced by changes in the average phonon amplitude. Deviations from this line correspond to effects of the isotopic disorder (gC).

and Γ_p is the phonon (HWHM) linewidth due to anharmonic decay. The real self-energy due to anharmonic decay has been included in ω and small corrections involving Π_i have been neglected in eq. (4b). The phonon self energy for natural germanium is given in fig. 2 of ref. [18].

3.2. Experimental results

Luminescence due to indirect recombination, as measured in ref. [13], gives information about the LA, TA and TO phonons at the L-point. These phonons exhibit between [72.6]Ge and [75.4]Ge a shift approximately equal to that required by the change in average mass. The accuracy of the measurements (~ 0.5 cm^{-1}), however, is just marginal for the purpose of detecting self-energy effects due to mass fluctuations.

These self-energies can be obtained for the optical phonons at Γ by means of Raman spectroscopy. $\Pi_r = +0.9 \pm 0.1$ cm^{-1} is found for natural [72.6]Ge [13,18], a value which compares reasonably well with the calculated $+1.5$ cm^{-1} [18]. Inelastic neutron scattering measurements on natural and isotopically pure samples are now being performed in order to obtain values of Π at other points of the Brillouin zone [19]. Two phonon-induced infrared absorption measurements, which are under way, should also give information about Π_r at several points of the Brillouin zone [20]. Second order Raman scattering has, so far, failed to give any conclusive results [18]. According to eq. (4), Π_i should be very small for the Raman phonons (Γ point of the BZ) since $\rho \approx 0$ at this point for $\Gamma_p \approx \Pi_i \approx 0$, Introducing into eq. (4) the value of Γ_p measured at low temperatures (0.49(5) cm^{-1}), we obtain a value of $\Pi_i = 0.0085$, for natural germanium, which should be hard to detect by comparison with an isotopically pure sample.

This value of Π_i is so small that the width of 'isotopically pure' [70]Ge actually even appears to be larger than that of the isotopically mixed [72.6]Ge. This apparent paradox arises from the fact that the width measured at low temperatures is due to anharmonic decay into two phonons. The probability for these processes is proportional to the squared amplitudes of the two modes into

which the Raman phonon decays, i.e., to $\overline{M}^{-1}$. The width of the Raman phonon in [70]Ge is thus expected to be larger than that of the natural [72.6]Ge since the variation in the anharmonic decay rate overcomes the effect of Π_i. We display in fig. 2 the measured dependence of 2Γ on $\overline{M}$ (dots) which can be written as [20]

$$2\Gamma = \left(A/\overline{M} \right) + \beta C, \tag{5}$$

where $A/\overline{M}$ represents the contribution of anharmonic decay and βC that of the self-energy due to isotopic disorder. The dashed line in fig. 2 represents the $A/\overline{M}$ contribution to eq. (2). Clearly, eq. (2) provides an excellent representation of the observed linewidths and βC is small, as discussed previously, and rather close to the calculated value ($\beta C = 0.017$ cm^{-1}).
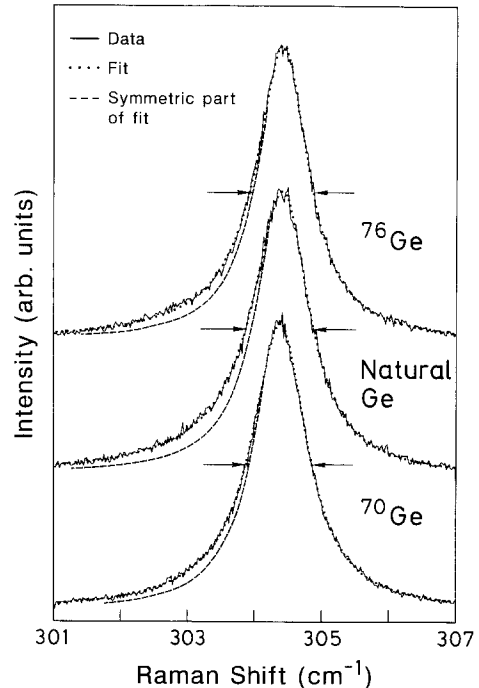

Fig. 3. Raman lines measured at 80 K with a high resolution spectrometer for the Γ-phonons of the three germanium samples of table 1. An Ar-ion laser line (5145 Å) was used. The jagged lines are experimental while the points represent fits with the asymmetric lineshapes described in the text. The dashed lines represent symmetric lineshapes. The horizontal scale corresponds to natural germanium, the other two spectra being shifted for display purposes [20].

We note that the decay times for non-equilibrium Raman phonons are given by $\tau = \Gamma/\pi$. Recent time-resolved Raman measurements confirm this relation between τ and Γ [21].

Figure 3 shows the observed Raman lineshapes for the Γ phonons of the three samples under consideration (solid lines). The frequencies have been shifted so as to place the peaks at the same position for ease of comparison. Note the asymmetry of the three peaks when compared with the dashed lines which would describe a symmetric shape. Natural Ge exhibits the largest asymmetry but the other two 'isotopically pure' samples also have asymmetric peaks. This asymmetry contains two contributions: The natural sample has a self-energy Π which, as given by eq. (4), is strongly asymmetric and an additional asymmetry due to a spread in k-vectors produced by the large absorption coefficients at the laser and scattering frequencies. The dotted line in fig. 3 has been calculated with these two contributions being included [20].

4. Conclusions

Isotopic disorder can affect significantly the spectra of vibronic and electronic elementary excitations in a crystalline solid. Germanium, with its five stable or nearly stable isotopes, is an ideal material for the investigation of isotope effects. Two types of effects can be distinguished: those which arise from the change in average phonon amplitude with isotopic mass and those produced by the random distributions of isotopes in natural or isotopically mixed samples. Among the first we have investigated the isotope effect on electronic excitation gaps and on phonon linewidths. Among the second, the corresponding complex self-energies (i.e., frequency shifts and broadenings) of phonons has been discussed. These effects may be important in a number of contexts, such as the lifetime of non-equilibrium phonons and the comparison of the frequencies of such phonons, and also the comparison of electronic excitations with results of 'ab initio' calculations.

References

[1] K. Grotz and H.V. Klapdor-Kleingrothaus, The Weak Interaction in Nuclear, Particle and Astrophysics, (Adam Hilger, Bristol, 1990);
N. Gehrels, Nucl. Instr. and Meth. A292 (1990) 505.

[2] H.J. Maris, Phys. Rev. B41 (1990) 9736.

[3] R.C. Buschert, A.E. Merlin, S. Pace, S. Rodriguez and M.H. Grimsditch, Phys. Rev. B38 (1988) 5219.

[4] J. Tauc and E. Antončík, Phys. Rev. Lett. 5 (1960) 253;
J. Tauc and E. Abrahám, J. Phys. Chem. Solids 20 (1961) 190;
J. Humlíček and F. Lukeš, Phys. Status Solidi (b)77 (1976) 731.

[5] J.C. Phillips, J. Phys. Chem. Solids 12 (1960) 208.

[6] D. Brust, J.C. Phillips and F. Bassani, Phys. Rev. Lett. 9 (1962) 94.

[7] L. Viña and M. Cardona, Phys. Rev. B34 (1986) 2586.

[8] D.E. Aspnes and A.A. Studna, Appl. Opt. 14 (1975) 220;
D.E. Aspnes, J. Opt. Soc. Am. 70 (1980) 1275.

[9] L. Viña, S. Logothetidis and M. Cardona, Phys. Rev. B30 (1984) 1979.

[10] P.B. Allen and M. Cardona, Phys. Rev. B27 (1983) 4760.

[11] P. Lautenschlager, P.B. Allen and M. Cardona, Phys. Rev. B31 (1985) 2163; 33 (1986) 5501.

[12] M. Cardona and S. Gopalan, in: Progress in Electron Properties of Solids, ed. R. Girlanda (Kluwer, Dordrecht, 1989) p. 51.

[13] V.F. Agekyan, V.M. Asnin, A.M. Krynkov, I.I. Markov, N.A. Rud', V.I. Stepanov and A.B. Churilov, Fiz. Tverd. Tela 31 (1989) 101 [Transl. Sov. Phys. Solid State 31 (1989) 12].

[14] S. Zollner, S. Gopalan and M. Cardona, Solid State Commun. 77 (1991) 485.

[15] A.T. Collins, S.C. Lawson, G. Davies and H. Kanda, Phys. Rev. Lett. 65 (1990) 891.

[16] S. Zollner, M. Cardona and S. Gopalan, Phys. Rev. B, in press.

[17] A. Mascarenhas, H. Katayama-Yoshida, J. Pankove and S.K. Deb, Phys. Rev. B39 (1989) 4999.

[18] H.D. Fuchs, C.H. Grein, C. Thomsen, M. Cardona, W.L. Hansen, E.E. Haller and K. Itoh, Phys. Rev. B43 (1991) 4835.

[19] L. Pintschovius, private communication.

[20] H.D. Fuchs, C.H. Grein, M. Bauer and M. Cardona, Phys. Rev. B, in press.

[21] H.D. Fuchs, C.H. Grein, R.I. Devlen, J. Kuhl and M. Cardona, Phys. Rev. B, in press.